ELSEVIER

PII: S0011-2275(98)00017-4

Cryogenics **38** (1998) 881–892

Printed in Great Britain
0011-2275/98/$—see front matter

Influence of thermal boundary resistance on bolometric response of high-T_c superconducting films

Jhy-Ping Wu*, Chia-Hung Shih and Hsin-Sen Chu

Department of Mechanical Engineering, National Chiao Tung University, Hsinchu, Taiwan 300, People's Republic of China

Received 24 July 1997

This work presents a thermal analysis on predicting the temperature increase and the voltage response of high-T_c superconducting bolometers. To consider the thermal boundary resistance between film and substrate, an acoustic mismatch model (AMM), a diffusive mismatch model (DMM), and an interfacial layer model (ILM) are employed. The thermal boundary resistance significantly influences the voltage response. Additionally, several common substrates are examined. $SrTiO_3$ (100) or $LaAlO_3$ (100) is a better substrate for high-T_c superconducting bolometers. Furthermore, we demonstrated that there are several factors to affect the voltage response, such as the pulse duration for a constant total incident energy or a fixed highest incident heat flux, the pulse distribution function in time, optical penetration depth, the thermal conductivities of the film and substrate, initial operating temperature, thickness ratio, and the amount of incident heat flux. One interesting finding was that when compared with experimental data, all the theoretical values from the present study as well as the other previously theoretical treatment overestimate the voltage response near the transition temperature.

Keywords: bolometer; thermal boundary resistance; voltage response

Nomenclature

B_s	elastic bulk modulus
c	specific heat
D	dimensionless thickness of substrate, d_s/d_f
d	thickness
g, g_o	heat generation by absorption, see Equation (7)
g_j	heat generation by Joule heating
h	Planck's constant = 6.6262×10^{-34} J s
$\hbar$	$h/(2\pi)$
I	bias current
J	current density
k	thermal conductivity
k_B	Boltzmann constant = 1.38062×10^{-23} J K^{-1}
N	number of atom of specimen
q	heat flux
q_b	boundary heat flux
q_i''	incident heat flux
R	electrical resistance
R_{bd}	thermal boundary resistance
r_d	thickness ratio of interfacial layer to film
r_k	thermal conductivity ratio of interfacial layer to film
T	temperature
T_{avg}	average film temperature
T_o	initial temperature
T_t	transition temperature
ΔT_{max}	maximum temperature change
t	time
t_p	pulse length
V	volume of specimen
v	voltage per unit volume
$\bar{v}$	sound velocity
x	distance from film front surface

Greek symbols

δ	skin depth
Γ	constant, see Equation (8)
γ	electrical resistivity
κ	constant, see Equation (8)
μ	permeability
σ	electrical conductivity
ρ	mass density
θ_D	Debye temperature
ω	angular frequency

Subscripts

		iter	iteration
		max	maximum
O	free space	*l*	interfacial layer
f	film	*s*	substrate

One of the most potential applications of high-temperature (high-T_c) superconducting thin films is a superconducting bolometer. Since the discovery of high-T_c superconductors, much effort has been focused on investigating the superconducting detectors[1–11], and several prototype bolometers have been designed and constructed[12–15]. A bolometer is a thermal detector of which resistance changes with incident radiation. Conventionally, detectors have been fabricated using semiconductors. Superconducting detectors have the following advantages over their semiconducting counterparts: less power required, faster response, lower noise, and greater bandwidth. However, expensive liquid helium and complicated cooling systems are required since detectors constructed from conventional (low-temperature) superconductors must be operated at liquid-helium temperature. In contrast, enormous advantages in simplicity of refrigerator and lower costs can be obtained since high-T_c superconducting detectors are operated at liquid-nitrogen temperature.

There are many interesting phenomena as the radiation is incident onto the superconducting film. An ideal superconductor, if operated at a temperature well below the transition temperature, is expected to be a perfect reflector of electromagnetic radiation at low-to-moderate frequencies[16]. The superconducting material will, however, absorb the electromagnetic radiation like a normal conductor if the energy associated with a particular photon frequency is greater than the energy gap of the superconductor. For radiation in infrared and visible regions, the photon energy is greater than the superconductor energy gap. When the radiation is incident onto the front surface of the superconducting film, the electromagnetic waves are simply absorbed and heat the lattice. Since the electrical conductivity is dependent on temperature, measurement of the electrical conductivity change is a measure of the absorbed energy. Detectors based on this effect are termed as bolometers.

The behavior of bolometers is generally divided into bolometric[1–4,7,8] and non-bolometric behavior[5,6,9–11,17,18]. In the bolometric (thermal) mechanism, the effect of the incident radiation is only heating and increases the temperature of the bolometer. In the non-bolometric case, the voltage response depends on a non-linearity in the voltage–current characteristic of the film[19]. The mechanism of this non-bolometric behavior is related to the creation of quasiparticle pairs induced by incident photons. To date, this non-bolometric effect has not yet been completely understood. Based on both mechanisms, several prototype bolometers have been designed and constructed[12–15]. A recent investigation[4] indicated that high-T_c superconducting bolometers based on the bolometric mechanism have a higher responsivity than those based on other mechanisms.

Besides the radiation absorption, the film energy will also increase through the imposition of bias current. When current flows through a conductor with resistance, the energy is dissipated in the conductor at a rate of I^2R or V^2/R if all the conductor is maintained at the same temperature, where V is the voltage. This dissipated energy is called Joule heat. The heat energy, as a whole, can be transmitted through a crystal via the motion of phonons, photons, free electrons, electron-hole pairs, or excitons. In most situations the heat conduction is carried mainly by the free electrons for metals but almost carried by the lattice vibrations (phonons) for non-metals. The high-T_c superconductors exhibit a surprisingly large phonon contribution to the heat flow that, in single crystal, amounts to some 60% and, in sintered samples, up to 90% of the total heat conduction[20]. On the other hand, the energy propagation through the substrate is only by phonons since most substrates are dielectric (insulating) materials. In brief, the energy propagation in the composite materials of the film and substrate is mainly by phonons. In generally, the absorption of substrate can be neglected because dielectric materials do not absorb the radiation at most wavelengths.

In modeling the heat transfer behavior of a superconducting bolometer subjected to incident radiation, two models have generally been utilized. The first is the surface heating model, which assumes that all of the energy is absorbed by the front surface of the superconducting bolometer and that there is no absorption of the incident energy within the film. The second is the heat generation model, in which the front surface is assumed to be adiabatic due to its small energy loss to the surroundings. The incident energy is absorbed within the whole film or part of the film. Chen *et al.*[21] had discussed the effect of skin depth, δ, on the heat transfer and compared between these two models in detail. The skin depth, δ, is a measure of the exponential penetration of plane electromagnetic waves into normal conductors. Actually, the surface heating model would be valid only when the skin depth is much smaller than the film thickness. Otherwise, the heat generation model should be employed. The influence of the skin depth on the voltage response with considering different thermal boundary-resistance models will be presented in this work.

In addition to the incident energy, the thermal boundary resistance between the superconducting film and the substrate also greatly affects the voltage response. Streiffer *et al.*[22] indicated that a significant thermal barrier exists at the Y-Ba-Cu-O/substrate interface. Marshall *et al.*[23] not only showed that a temperature-dependent thermal barrier significantly restricts heat transfer from the film into the substrate, but also quantified this thermal boundary resistance. Marshall *et al.*[23] stated that the rate of flow through the Y-Ba-Cu-O/MgO interface is about 100 times less than the rate of flow in the Y-Ba-Cu-O film. Moreover, the barrier to thermal flow at the MgO substrate interface has a thickness of the order of the unit-cell size of ~ 1.1 nm. At present, there are at least three different models used for predicting the thermal boundary resistance. The first model is assumed with a radiation boundary condition, where the thermal flow across the interface is proportional to the difference of the fourth power of the temperature on each side of the interface[24]. This approximation is based on the

*To whom correspondence should be addressed. E-mail: hachu@cc.nctu.edu.tw; Fax: 886-3-5727930.

acoustic mismatch model (AMM). Since the temperature difference between the two materials is usually much smaller than the mean temperature of the two sides, the thermal flow across the interface is approximately proportional to the temperature difference, i.e. the thermal boundary resistance R_{bd} is inversely proportional to the cubic power of the mean temperature. However, the AMM is found to be in agreement with measurements only for temperatures below ~ 30 K[25]. When the temperature increases, the thermal boundary resistance does not continue to decrease with T^3, but instead approaches a constant value at higher temperatures. For some situations, if the interface itself is a very strong diffuse scatterer of phonons, the implicit assumptions of the AMM, based on that phonons either reflect specularly or refract "specularly", are thus certainly not satisfied. Instead, the implicit assumption of complete specularity is replaced with the opposite assumption, that all the phonons are diffusely scattered at the interface. Therefore, the second model named diffusive mismatch model (DMM)[25] assumes that acoustic effects at interfaces to be destroyed by diffuse scattering, so that only aspect of the AMM which must be modified in the DMM is the transmission probability. The third model (the interfacial layer model, ILM) assumes an interfacial layer of a variable thickness inside the superconducting film, where the diffusivity is significantly lower (~ 10–100 times) than that of bulk Y-Ba-Cu-O[23], since Nahum *et al.*[26] recently measured the thermal boundary resistance between $YBa_2Cu_3O_{7-\delta}$ thin film and several substrates and found the measured thermal boundary resistance to be a factor of ~ 80 larger than the resistance derived from the AMM at 100 K.

Another important factor influencing the thermal behavior and the voltage response of high-T_c superconducting bolometers is the substrate properties. The most common substrates used to fabricate high-T_c superconducting bolometers are MgO, $SrTiO_3$, $LaAlO_3$, sapphire (Al_2O_3), and ZrO_2. The effect of these substrates on the temperature increase is considered in this study.

An adequate thermal model is crucial to the prediction of the temperature rise of high-T_c superconducting bolometers. Superconducting bolometers are based on steep temperature-dependent resistance at the transition temperature. Hence, a slight temperature rise will cause a large resistance change and then a large voltage change. For typical bolometers, the temperature change is controlled to be within 0.01 K. Some superconducting bolometers even require the temperature change to be within 0.001 K. Therefore, a correct prediction of the temperature is very important. Three previously theoretical investigations did give fair analysis. Kumar and Joshi[27] presented a bolometric study of examining the effects of incoming radiation flux and bias current on the sensitivity and response of a bolometer. Joule heating was considered in their work. However, they did not consider thermal boundary resistance, which several papers have proved to be very important. Flik *et al.*[28] presented a rigorous thermal analysis of superconducting bolometers. They considered a conjugate radiation/conduction problem. They also considered the effects of variable properties of the film and the substrate as well as thermal boundary resistance based on the AMM. Yet they did not consider Joule heating, which is generally very important in predicting the performance of bolometers. Furthermore, they employed the AMM, which underestimates the thermal boundary resistance at above ~ 30 K, to examine the effects of thermal boundary resistance. In addition to the above researches, Chen *et al.*[21] further considered simultaneously two different thermal boundary resistance, the AMM and the ILM, to analyse the voltage response of high-T_c superconducting bolometers. They concluded that the thermal boundary resistance significantly influences the voltage response and different model can induce the obvious deviation in the special temperature range.

This paper presents a heat transfer analysis considering the other thermal boundary-resistance model (DMM) to investigate the voltage response of the superconducting bolometers. Variable properties, conjugate film/substrate conduction equations, Joule heating, and the effect of different substrates are taken into account. Both the AMM and the ILM are also employed to compare with the DMM to examine the effects of different thermal boundary-resistance models on the voltage response of bolometers. The analysis is applied to an incident pulse, which is absorbed within a skin depth. Our results show that the thermal boundary resistance, the type and magnitude of incident heat flux, and the thermal properties of the film and substrate have a great influence on the temperature increase and the performance of a high-T_c superconducting bolometer, whereas the effects of penetration depth and substrate thickness on the voltage response are more insignificant than the others. From the viewpoint of heat transfer, $SrTiO_3$ (100) or $LaAlO_3$ (100) is a better substrate for fabricating high-T_c superconducting bolometers. However, at temperatures near the transition temperature, the calculated voltage responses in this study as well as the previous rigorous thermal analysis in Chen *et al.*[21] are higher than those obtained by experimental measurements.

Analysis

A superconducting bolometer can be simply described as a superconducting film deposited on a substrate, as shown in *Figure 1*. Typically, the film thickness, d_f, is from 0.01 to 1 μm, and substrate thickness, d_s is either 1 or 0.5 mm, i.e. several hundred or even hundred thousand times thicker than the thin film.

The influence of Joule heating on bolometric response has been discussed in detail by previous researchers[21,28]. Once Joule heating is neglected, it leads to a smaller predicted temperature rise. A criterion for this effect to be neg-

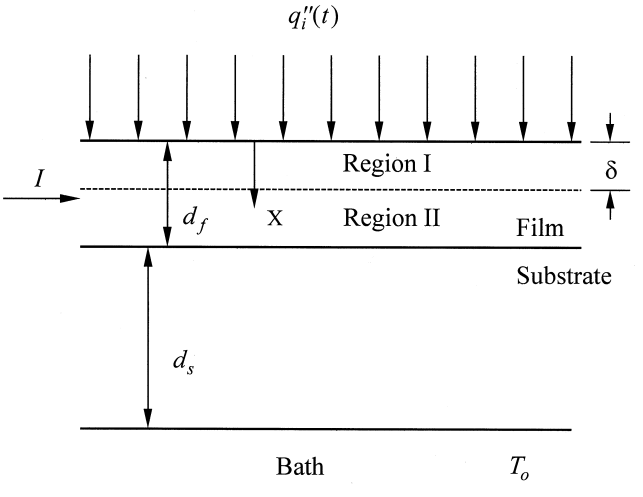

Figure 1 Schematic diagram of the physical system

ligible is that the Joule heating power must be smaller than the time rate of change of thermal energy stored in the film, $I^2R \ll \rho_f c_f \Delta T_{max}/t_p$, where R is the electrical resistance and ΔT_{max} the maximum temperature change during the transient. Referring to the experimental results of Frenkel *et al.*[5] for t_p = 200 ns and I = 5 mA, this condition is found to be well satisfied for T_o = 50 K, but not for T_o = 70 K. At low temperatures, where the $R-T$ curve is in the flat region, Joule heating can be neglected. At high temperatures, where the $R-T$ curve is in the steep region or on the plateau, the neglect of Joule heating leads to an underestimation of the bolometric response.

If the whole film were at the same temperature, the Joule heating would be equal to I^2R. However, the temperature of the film at the x direction is not constant during the conduction transient. Therefore by considering the film to be composed of infinitely many filaments and each filament in the film to be in parallel, the voltage change per unit length v is given as[27]

$$v = Jd_f\left[\int_0^{d_f} \frac{dx}{\gamma(T(x))}\right]^{-1} \tag{1}$$

where γ is the resistivity and is equal to resistance times unit cross-sectional area normal to the current per unit length, and J is the current density. The local Joule heat per unit volume g_j is equal to the square of the voltage changes per unit length divided by the resistivity, and can be represented as follows:

$$g_j = \frac{(Jd_f)^2}{\gamma(I,T_f)}\left[\int_0^{d_f} \frac{dx}{\gamma(I,T_f)}\right]^{-2}. \tag{2}$$

The skin depth, δ, is given as[29]

$$\delta = \sqrt{\frac{2}{\omega\mu\sigma}}, \tag{3}$$

where ω is the angular frequency, μ the permeability of the medium penetrated by the electromagnetic wave, and σ the electrical conductivity. For most materials, $\mu \sim \mu_0$, i.e. the permeability of free space. A typical skin depth for an infrared source is about 0.1–1 μm. This skin depth, in fact, determines the validity of the surface heating model. Only when the skin depth δ is much smaller than the film thickness is the surface heating model valid. Currently, Chen *et al.*[21] presented that the surface heating model overestimates the temperature increase. Since superconducting bolometers are generally operated at the transition temperature, a slight temperature increase will cause a large voltage response. To predict the voltage response correctly, they suggest that the effect of the skin depth should be considered in a heat transfer analysis of superconducting bolometers. Consequently, to assume that all incident energy is absorbed within a skin depth of the film. The energy equations, initial conditions, and boundary conditions are as follows:

$$\rho_f c_f \frac{\partial T_f}{\partial t} = \frac{\partial}{\partial x}\left(k_f \frac{\partial T_f}{\partial x}\right) + g(x,t) + \frac{(Jd_f)^2}{\gamma(I,T_f)}\left[\int_0^{d_f} \frac{dx}{\gamma(I,T_f)}\right]^{-2} \tag{4a}$$

$$\rho_s c_s \frac{\partial T_s}{\partial t} = \frac{\partial}{\partial x}\left(k_s \frac{\partial T_s}{\partial x}\right), \tag{4b}$$

$$T_f(x,t=0) = T_s(x,t=0) = T_o, \tag{5}$$

$$\frac{\partial T_f(x=0,t)}{\partial x} = 0 \tag{6a}$$

$$-k_f \frac{\partial T_f}{\partial x}(x=d_f,t) = -k_s \frac{\partial T_f}{\partial x}(x=d_f,t) \tag{6b}$$

$$-k_f \frac{\partial T_f}{\partial x}(x=d_f,t) = q_b(t) \tag{6c}$$

$$T_s(x=d_f+d_s,t) \rightarrow T_o, \tag{6d}$$

where T is the temperature, ρ the density, c the specific heat, and k the thermal conductivity. Subscripts f and s stand for the film and the substrate, respectively. $g(x,t)$ represents volumetric heat generation. Uniform or constant heat generation is usually assumed. In this work, however, we consider the effect of the skin depth δ, and thus the volumetric heat generation is expressed as

$$g(x,t) = g_o(t)\exp(-x/\delta). \tag{7}$$

This generation form is not given arbitrarily, but is from Beer's law.

If the AMM or the DMM model is employed for the boundary condition of the interface, Equation (6c) becomes

$$-k_f \frac{\partial T_f}{\partial x}(x=d_f,t) = \kappa\{[T_f(x=d_f,t)]^4 - [T_s(x=d_f,t)]^4\} \tag{6c'}$$

$$\kappa = \frac{2\pi k_B^4 \Gamma}{h^3 \bar{v}^2}\left(\frac{\pi^4}{15}\right), \tag{8}$$

where κ is a constant which depends on the densities and the longitudinal and transversal sound velocities. Suppose there were no thermal boundary resistance between the superconducting thin film and substrate, the characteristic time required for thermal diffusion across the film thickness would be proportional to the square of the film thickness. There is a significant thermal boundary resistance to prevent thermal flow from removing out the film, however, and this characteristic time is found to be linearly proportional to the film thickness[23]. Furthermore, Chen *et al.*[21] indicated that neglecting the thermal boundary resistance causes the average film temperature to be greatly underestimated. Here, there are three different thermal boundary-resistance models applied to the interface between the film and the substrate to be proposed to analyse the voltage response of a bolometer.

Acoustic mismatch model (AMM)[24]. Predictions based on this model are found to be in agreement with measurements below 30 K. The expression for this boundary condition is given in Equation (6c)′ and Equation (8). The most important constant is Γ, a function of the material

properties of the two contacting media. Using the figure provided by Little[24], Γ can be obtained if the density ratio and the sound velocity ratio of two media are known. To the authors' knowledge, no direct measurements have been made for the average sound velocities of some typical substrates. However, there are at least two ways to find the sound velocity. The first way is from the elastic bulk modulus[30], B_s.

$$\bar{\nu} = \sqrt{\frac{B_s}{\rho}} \tag{9}$$

For solids, Equation (9) gives the correct order of magnitude for the longitudinal sound velocity. Comparison with direct measurements shows that sound velocities calculated from the elastic bulk modulus give tolerably favorable values for some typical solids and demonstrates that sound velocities are of the order of 5000 m/s in typical metallic, covalent, and ionic solids. The second method is from the Debye temperature[30,31], θ_D:

$$\bar{\nu} = \frac{k_B \theta_D}{\hbar} \left(6\pi^2 \frac{N}{\overline{V}} \right)^{-1/3} \tag{10}$$

where $\hbar = h/(2\pi)$, $\overline{V}$ is the volume of the specimen, and N is the number of atoms of the specimen. For MgO, $\overline{V}/N$ = 0.935 nm. Substituting this value and θ_D = 946 K [32] into Equation (13), we obtain $\bar{\nu} \sim$ 6700 m/s, about 4% lower than the value reported by Slack[33].

Diffusive mismatch model (DMM) [24]*.* This model is chosen in order to suggest the basis of the model and to contrast that with the basis of the AMM. In this model, acoustic effects at interfaces are assumed to be destroyed by diffuse scattering, so that the only determinant of the transmission probability is densities of states and detailed balance. In other words, the only aspect of the AMM which must be modified in the DMM is the transmission probability. Therefore, Equation (6c)′ and Equation (8) are applicable to this model but the value of Γ is different with that derived from the AMM, which is based on that phonons either reflect specularly or refract "specularly".

Interfacial layer model. The thermal boundary resistance between solids is often actually higher than that calculated from the AMM. Thus, it is important to find a model that can predict the thermal boundary resistance more accurately. The other model for calculating thermal boundary resistance is the interfacial-layer model (ILM)[23]. This model assumes a layer of a variable thickness (~ 1–10% of the total sample thickness) inside the Y-Ba-Cu-O film, where the diffusivity is significantly lower (~ 10–100 times) than that of bulk Y-Ba-Cu-O. Based on the experimental results of Marshall *et al.*[23], the conductivity ratio of interfacial layer to film is assigned to be 0.01 and the interfacial layer thickness is assigned to be 1.1 nm. According to this concept, an interfacial layer is assumed to exist between the film and the substrate, and its energy equation, initial, and boundary conditions are as follows[21]:

$$\rho_f c_f \frac{\partial T_l}{\partial t} = \frac{\partial}{\partial x} \left(r_k k_f \frac{\partial T_l}{\partial x} \right), \tag{11}$$

$$T_l = T_o, \text{ at } t = 0 \tag{12}$$

$$T_f = T_l, -\frac{\partial T_f}{\partial x} = -r_k \frac{\partial T_l}{\partial x} \text{ at } x = d_f \tag{13}$$

$$T_l = T_s, -r_k k_f \frac{\partial T_l}{\partial x} = -k_s \frac{\partial T_s}{\partial x} \text{ at } x = d_f(1 + r_d) \tag{14}$$

where r_k is the thermal conductivity ratio of the layer to the film, r_d the thickness ratio of the layer to the film, and subscript l represents the layer.

This model can be significantly influenced by the assumptions of the values of r_k and r_d. If r_k decreases, i.e. the thermal conductivity of the interfacial layer is decreased, the effect of a resistance would be more apparent. Whereas as r_d or the thickness of the interfacial layer increases, the temperature gradient at the interface can be attenuated, on the contrary, once r_d decreases, the temperature change from film to substrate would be more fluent. Therefore, the precise estimation of r_k and r_d is correspondingly important by various experiments, while these parameters are strongly dependent on the material categories, thus resulting in difficulty in estimating these parameters for the universal material.

Method of solution

Since Joule heating is a complicated function of film temperature, the film energy equation is highly non-linear. We will use a fully implicit, finite-difference scheme with an under-relaxation technique to solve this highly non-linear conjugate film/substrate conduction problem. Harmonic mean is employed to model the non-uniform thermal conductivities. Iterations between the Joule heating, thermal properties, and energy equation at each time step continue until the criterion of convergence, $|T - T_{iter}|/|T_{max}|$, is within 10^{-4}. Low temperature cases require the use of a smaller relaxation factor and thus take more time to calculate. If the ILM is employed as the interfacial boundary condition, the convergence of numerical calculations is swifter than that calculated from the AMM or the DMM, because the assumption of continuous temperature is given at the interface between different layers for the ILM.

Results and discussion

To compare our results with those of previous investigations, the configuration of the bolometer is chosen to be the same as those from the experimental work of Frenkel *et al.*[34] and two theoretical analyses in Flik *et al.*[28] and Chen *et al.*[21]. The thin-film superconductor is Y-Ba-Cu-O with a thickness of 40 nm deposited on the MgO substrate. The bias current is 5 mA. The incident heat flux for the 200 ns long pulse is represented as[28]

$$q_i'' = (3.81 \times 10^7) \exp\left[\frac{-(t/t_p - 1)^2}{0.36067} \right]. \tag{15}$$

The energy absorbed equals the absorptance times incident energy. The absorptance is 0.23[28]. Regarding the thermal boundary resistance in the base case, the values of Γ are 0.2 and 0.131 for the AMM and the DMM, respectively, as calculated using the figure provided by Little[24]. For the ILM, Marshall *et al.*[23] stated that the rate of flow across

the Y-Ba-Cu-O/MgO interface is ~ 100 times lower than the rate of flow across the Y-Ba-Cu-O film. This finding corresponds to the case where the conductivity ratio r_k of interfacial layer to film is 0.01. In addition, we assume the thickness ratio r_d is assumed herein to be 0.025. The fact that the surface heating model neglects the effect of the skin depth accounts for why the following results were all obtained by employing the heat generation model.

Temperature profile

Figure 2 displays the temperature profiles across the film and partially into the substrate at the initial temperature T_o = 50 K with a substrate thickness of 1 mm. Incident total energy is persistently equal to 7.96 J/m^2 and heat flux q_i'' reaches a maximum at 200 ns. The temperature profiles, however, do not reach their maximum average film temperature, i.e. T_{avg}, at t = 200 ns (the time of the incident energy arriving at the maximum value, but until t = 220 ns) since the energy needs time to transfer to the entire film to obtain a higher average temperature within a larger diffuse region before more heat is conducted into the substrate. "Delay time" refers to the difference in time between the maximum incident energy and the maximum film average temperature. The temperature decreases with distance into the substrate. At the interface a great temperature jump occurs. Moreover, the fact that heat conductance across the film is larger than the heat conductance across the interface accounts for why the temperature difference across the interface is larger than that across the film. Another notable phenomenon is the linear tendency of the temperature profiles. In general, temperature profiles governed by transient heat conduction are curved, and are linear only for steady states without heat generation. From a mathematical perspective, the criterion for linearity is $\rho_f c_f \partial T/\partial t \ll k_f \partial^2 T/\partial x^2$. By substituting the characteristic values of ρ_f, c_f, k_f, d_f, and t_p = 200 ns, this criterion is found to be well satisfied. From a heat transfer perspective, on the other hand, the time required for thermal diffusion across the film thickness is ~ 0.5 ns. *Figure 2* plots the times of at least 50 ns. For these times, the film is in a relatively steady state, causing the linearity of the temperature profile.

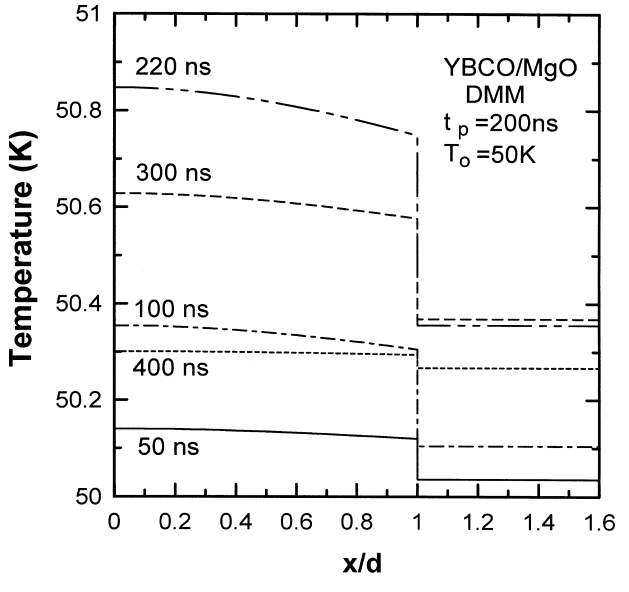

Figure 2 Transient temperature profiles across the film and the interface, and partially into the substrate for DMM

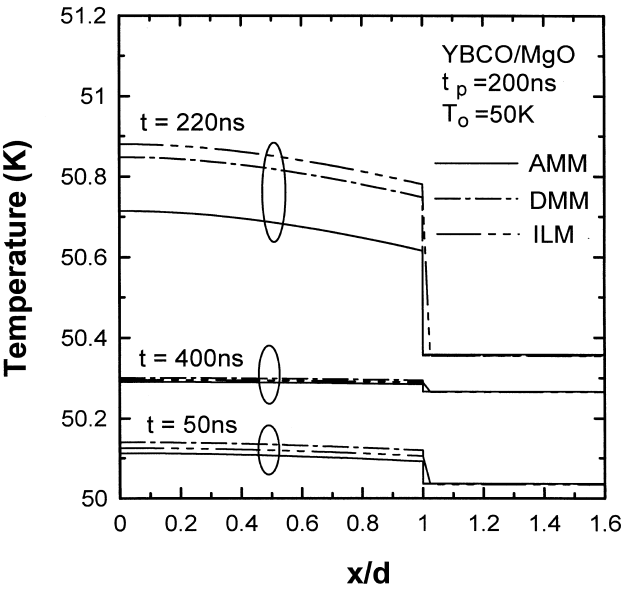

Figure 3 Effect of different thermal-boundary-resistance models on transient temperature profiles

Figures 3 and *4* compare the results of three different models for thermal boundary resistance. Notably, the temperature profiles at the interface for the ILM are continuous since an interfacial layer is assumed to have a continuous temperature at the boundaries; however, the profiles exhibit a significant temperature difference as the results consider the other thermal boundary-resistance models. From a heat transfer perspective, a greater thermal resistance impedes the more energy to transfer through the substrate into the coolant. Therefore, at the same time in *Figure 3*, the temperature profiles of the DMM always exceeds that of the AMM, because the thermal resistance value for the DMM is greater than that for the AMM for all temperatures. Besides, the magnitude of thermal resistance predicted by the ILM is maintained as a constant during all time, whereas the others models, i.e. AMM and DMM, predict a variable resistance with temperature. That is, the resistance decreases with an increasing temperature. According to

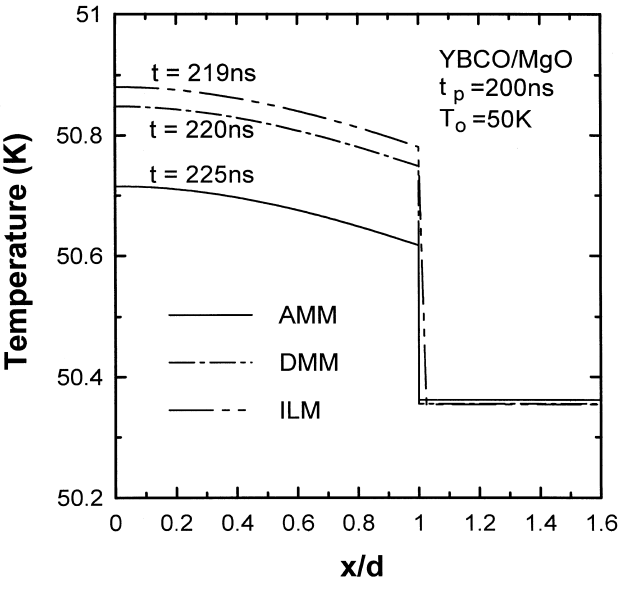

Figure 4 Comparison of different thermal-boundary-resistance models at the maximum average temperature

Equation (6c)′, for small values of the ratio $(T_f - T_s)/T_f$, Equation (6c)′ can be written as

$$q = 4\kappa T_f^3 (T_f - T_s) \tag{16}$$

which yields a simple formula for the thermal boundary resistance, $R_{bd} = 1/(4\kappa T_f^3)$. Such a relation indicates that the boundary resistance due to an acoustic mismatch is inversely proportional to the third powers of the thin-film temperature. Consequently, *Figure 3* reveals that when the film temperatures are lower at $t = 50$ and 400 ns, the temperature difference across the interfacial layer calculated from the ILM is the magnitude between those from the AMM and the DMM. This observation suggests that at these times the thermal boundary resistances for the ILM cases are greater than those for AMM, but lower than those for DMM. As the film temperature increases, the resistance of the ILM can surpass that of the DMM in magnitude, as shown in *Figure 3* at $t = 220$ ns. This figure also indicates that the film temperatures are nearly independent of the type of resistance due to two factors: (a) the substrate thickness is markedly larger than that of the film; and (b) the incident energy is insufficient to influence heavily the temperature distribution of the substrate.

In bolometer-related applications of priority concern is the magnitude of the maximum voltage response, which is proportional to the maximum average temperature of the film. According to *Figure 4*, the maximum average temperatures of the film reach the different values at different times for the three resistance models. The temperature increase for ILM is the highest, that for DMM is the second, and that for AMM is the lowest. Interestingly, the larger resistance not only induces an increase of the temperature difference across the interface, but also shortens the delay time. The delay times are 19, 20, and 25 ns, for the ILM, the DMM, and the AMM, respectively. A delay time is attributed primarily to the capability of heat transfer of a substrate, which can bring out the energy from the film before the energy accumulated in the film can induce a maximum average temperature.

Incident pulse

Figure 5 demonstrates how the thermal boundary resistance influences the voltage response for various pulse durations, t_p. The energy flux and bias current are fixed at 7.96 Jm^{-2} and 5 mA, respectively. The voltage response increases with a decreasing pulse duration for all resistance models. Because of the incident total energy fixed, a shorter pulse produces a greater average incident heat flux, leading to a greater average temperature increase and voltage response. Restated, a more concentrated energy released within a shorter duration can cause the energy to diffuse more rapidly over the entire film, whereas the voltage responses for three different resistance models approach the same limiting constant for a shorter duration, which is equivalent to about 2000 mV. This result is largely attributed to the fact that the time to arrive at the maximum film average temperature is shorter than that of a sensible amount of energy transferred through an interfacial layer into the substrate. Therefore, a limiting voltage response exists in this bolometer for a fixed amount of incident energy; under this situation, the maximum voltage response of a bolometer is independent of the pulse duration, the magnitude of thermal boundary resistance, and substrate effects. Restated, the

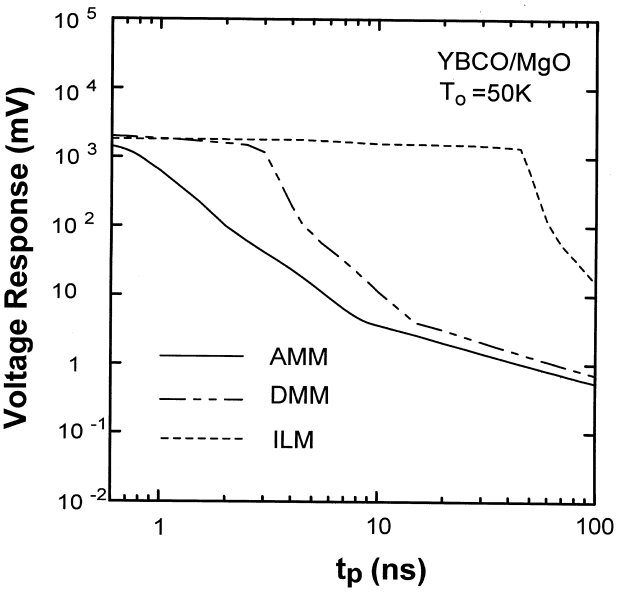

Figure 5 Variation of maximum voltage response with pulse duration at a constant incident total energy for different thermal-boundary-resistance models

effect of thermal boundary resistance is attenuated with a decrease in pulse duration. The limiting values are approximately 4.5×10^{-8}, 10^{-9}, and 6×10^{-10} s, respectively, for the DMM, the ILM, and the AMM. Above the limiting value, the voltage response relies heavily on the length of pulse duration. For instance, the voltage response is about 0.5 mV at $t_p = 100$ ns for the AMM case; however, once t_p decreases to 1 ns, the voltage response rapidly increases about 2600 times to 1300 mV. When the pulse duration increases persistently, the voltage response can decrease until zero with a fixed incident energy.

This study also attempts to understand further how different modeling functions influence the performance of a superconducting bolometer by using three different functions to model the incident heat flux. In addition to the Gaussian distribution with respect to time, the sine function and unit step function are also chosen to demonstrate the effects of κ on voltage response, as shown in *Figure 6*. Where κ represents a parameter, and is inversely proportional as increasing κ decreases R_{bd}. The energy distributions of the three selected functions show that the Gaussian distribution possesses the most concentrated energy among all functions during the incidence of the pulse, the next is the sine function and, finally, the unit step function, which evenly distributes the energy. As *Figure 5* indicates, the more concentrated the energy generally leads to a larger voltage response. Consequently, this figure reveals that an incident heat flux with a higher peak value yields a higher voltage response, in spite of the equal incident energy per unit area and the same thermal boundary resistance. In particular, the voltage responses for unit step function are always below the others far away. Thus, according to our results, the form of an incident heat flux can significantly influence the response of a bolometer. Another noteworthy phenomenon is that as κ increases, i.e. R_{bd} decreases, the voltage response decreases asymptotically towards a smaller constant since a lower R_{bd} prevents the energy from more easily accumulating within the film, ultimately resulting in the poor performance and sensitivity of a bolometer.

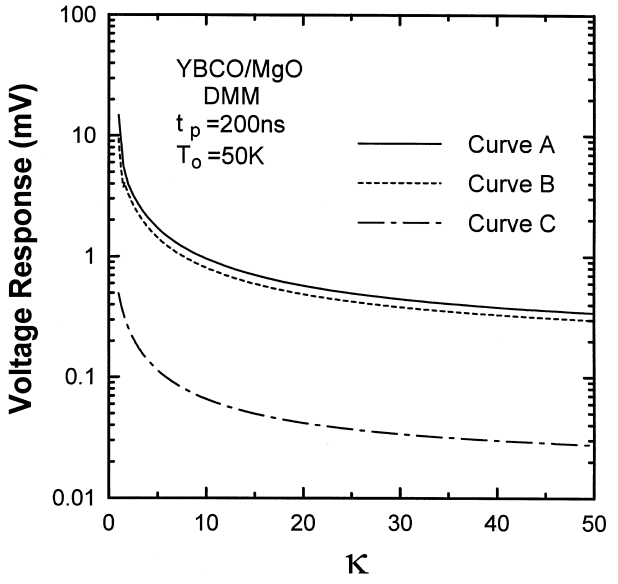

Figure 6 Variation of maximum voltage response with κ for the incident pulse in different distribution functions with respect to time. Curve A, Gaussian distribution; curve B, sine function; curve C, unit step function

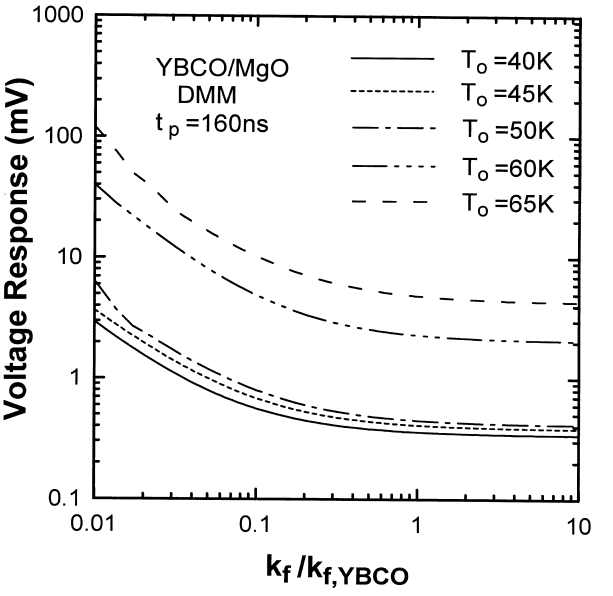

Figure 8 Variation of maximum voltage response with the ratio of thermal conductivity of selected film to YBCO at 50 K for different initial operating temperatures

Thermal property

Another probable factor to impact the bolometer response is the optical penetration depth, δ, which depends on the wavelength of an incident electromagnetic wave and the film properties. *Figure 7* depicts the influence of penetration depth on voltage response while considering the DMM for different pulse durations, t_p = 160, 200 and 400 ns. At the special pulse duration with a fixed energy, the smaller penetration depth implies a lower voltage response since the incident energy is released within a thinner region adjacent to the upper surface. This finding suggests that the energy distributes itself over a smaller volume to yield a lower average film temperature, whereas the effects of penetration depth on the performance of a bolometer are insignificant and only generate a diminutive decrease in voltage response for a smaller δ. This result implies that, for these pulse durations, when $\delta/d_f > 0.1$, the voltage responses reach different constants and the influence of penetration depth can be neglected. This figure also indicates that a shorter pulse leads to a greater average temperature increase and voltage response, as previously discussed in *Figure 5*. Notably, if the pulse duration decreases for the same incident energy, the effects of penetration depth can be slightly strengthened, particularly in a thinner penetration depth.

Figures 8 and *9* illustrate the variation of voltage response with different thermal conductivity ratios of the film and substrate, respectively, for various initial operating temperatures. Herein, we select the base thermal conductivity for the superconducting film YBCO[35], k_f = 2 $Wm^{-1}K^{-1}$, and the substrate MgO, k_s = 1088 $Wm^{-1}K^{-1}$, at

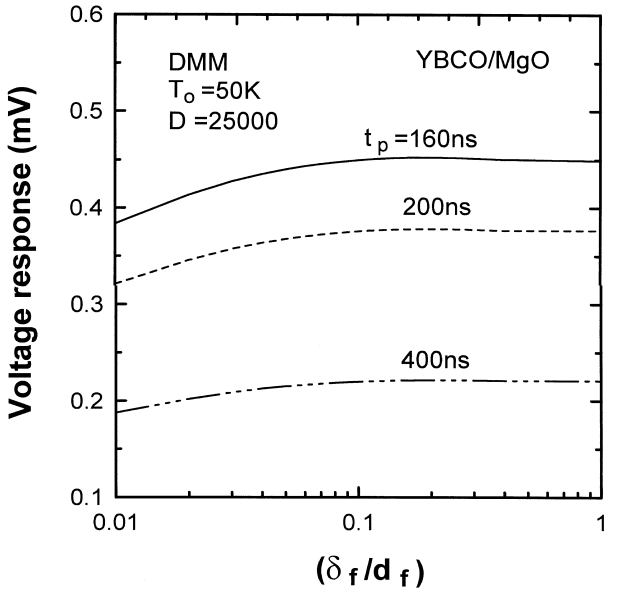

Figure 7 Variation of maximum voltage response with the ratio of penetration depth to film thickness for different pulse durations

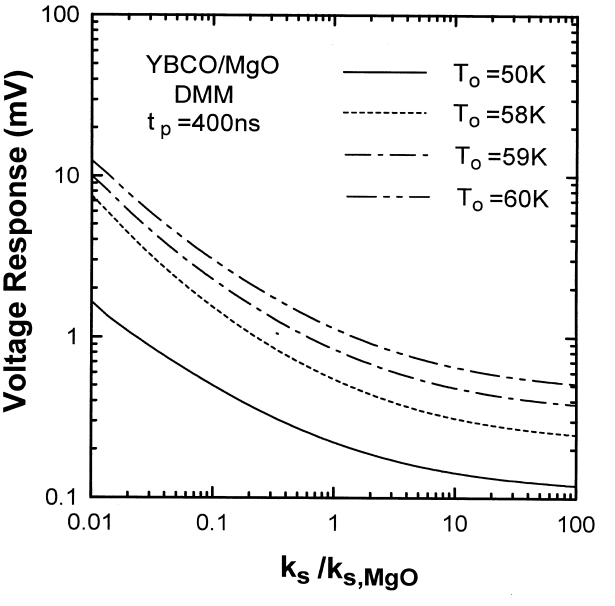

Figure 9 Variation of maximum voltage response with the ratio of thermal conductivity of selected substrate to MgO at 50 K for different initial operating temperatures

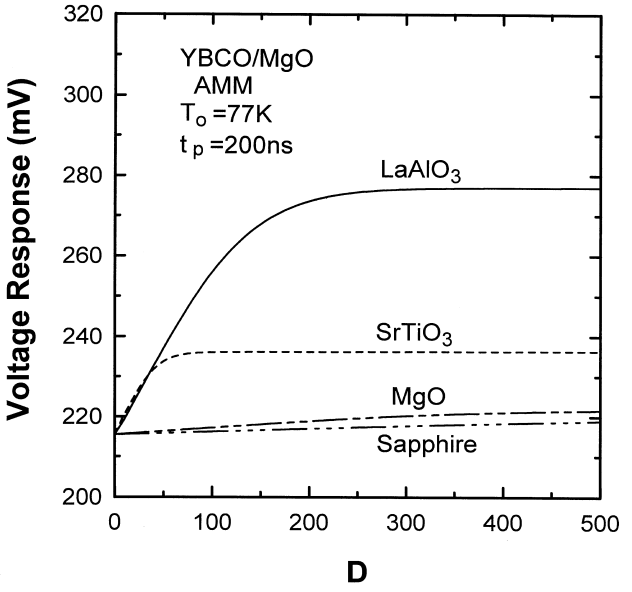

Figure 10 Comparison of different substrates on maximum voltage response with various dimensionless thicknesses of substrates

T_o = 50 K. According to those results, the voltage response for a higher T_o surpasses that for a lower T_o for all the conductivity ratios until the maximum response occurs, as mentioned later in *Figure 13*. Two main factors lead to these results. One is that dR/dT increases with T_o for $T_o \leq$ 77 K, as shown in *Figure 13*. Another factor is that the thermal boundary resistance based on the DMM depends on temperature. The thermal boundary resistance at a lower T_o is greater than that at a higher for the DMM, and causes a greater average film temperature when this factor overwhelms the others. In addition, the magnitude of voltage response increase is nearly independent of the two thermal conductivities within the entire calculating conductivity range. Restated, the effects of thermal conductivity do not change when varying the initial operating temperature.

For Y-Ba-Cu-O films, the most common substrates used for fabricating superconducting bolometers are MgO, $SrTiO_3$, sapphire, and $LaAlO_3$. In this work, we examine the effects of these different substrates by employing the AMM. *Figure 10* demonstrates how different substrates influence the voltage response for various thicknesses of the substrate at T_o = 77 K and t_p = 200 ns. *Table 1* lists the properties of substrates at 77 K. In general, increasing the substrate's thickness can induce not only a higher capacity of heat, but also a weaker capability of heat transfer. Such an increase reduces the substrate temperature and, hence, makes the heat transfer more difficult from the substrate to the coolant, particularly for a lower thermal conductivity of a substrate, such as $LaAlO_3$ and $SrTiO_3$. Consequently, the fact that the voltage response is approximately proportional to the temperature increase accounts for why it increases with an increasing D. For $LaAlO_3$ and $SrTiO_3$ substrates, the voltage response quickly approaches a maximum constant due to the lower thermal conductivity to form an analogically larger capacity of heat. In contrast, for MgO and sapphire with a large thermal conductivity, the voltage response only slightly increases with D until 500, because the heat generated within the film rapidly removed to a coolant through the substrate. On the other hand, the voltage responses for all substrates reach the same value as D = 0 with no substrate. When D > 50, the voltage response for $LaAlO_3$ is the highest; that for $SrTiO_3$ is the second; that for MgO is the third highest; and that for sapphire is the lowest. Several factors lead to this result. The thermal conductivity and the specific heat of the substrates significantly influence the temperature increase of the film. A high thermal conductivity conducts heat more rapidly to the coolant, thereby reducing the temperature increase of the film. A substrate with a lower heat capacity has a higher voltage response owing to the fact that the lower the heat capacity implies an increasing substrate temperature. This result subsequently leads to a smaller temperature difference between the film and the substrate, thereby complicating the conducting of heat from the film to the substrate. The heat capacity of $LaAlO_3$ is approximately 13 times smaller than that of $SrTiO_3$, slightly influencing the temperature increase of the film for the lower D and strongly inducing the difference between the two materials with 40 mV for the higher D. In contrast, the thermal conductivity of $SrTiO_3$ is slightly lower than that of $LaAlO_3$; this lower thermal conductivity magnifies the temperature increase of the film. Such an effect appears visibly in the range of D < 50. Under this range, the influence of thermal conductivity overwhelms that of the heat capacity and, thus, the voltage response of $SrTiO_3$ exceeds that of the $LaAlO_3$. The film's voltage response is lowest for sapphire, owing to its extremely high thermal conductivity. Another potential substrate is ZrO_2. Owing to the unavailability of data on the thermal conductivity of ZrO_2 at low temperatures, the temperature increase cannot be predicted. Zheng *et al.*[11] reported a value of 1.5 W m^{-1} K^{-1}. This low thermal conductivity is rather favorable for the temperature increase and voltage response. However, this value is questionable. In this work, for all the analysed substrates the preferable substrate to enhance the responsivity of the bolometer appears to be $LaAlO_3$.

Table 1 Properties of substrates at T_o = 77 K

T_o = 77 K	ρ_s (g/cm^3)	k_s (W/m K)	C_s (J/Kg K)	$\bar{v}$ (m/s)	Γ[a]
$LaAlO_3$	6.52[b]	18.6[b]	14.1[b]	5400[b]	0.3
$SrTiO_3$	5.12[d]	18.3[c]	181.6[c]	7200[d]	0.15
Sapphire	3.99[e]	1131[c]	60.7[c]	6600[e]	0.2
MgO	3.58[e]	485.7[e]	88.7[c]	7000[e]	0.2

[a]From figure provided by Little[24].
[b]Michael *et al.*[37].
[c]Touloukian and Dewitt[38].
[d]Calculated from Young's modulus, Nassau and Miller[39].
[e]Slack[33].

Incident heat flux

Figure 11 illustrates the effects of incident heat flux with the DMM for t_p = 200 ns. As easily understood, the voltage response increases with an increase in the incident heat flux since a greater amount of energy irradiated into the film increases the maximum average temperature. For instance, for T_o = 50 K the incident heat flux changes from 1 to 100 Wm^{-2} and, then, the voltage response increases slightly from 0.06 to 5 mV. On the other hand, for T_o = 55 K when the heat flux exceeds 40 Wm^{-2}, the response rises more strongly up to 17 mV for incident heat flux 100 Wm^{-2}. This abrupt increase is because beyond the flux, 40 Wm^{-2}, the increase of film temperature approaches its transition temperature, i.e. in the vicinity of the critical temperature of a superconductor, where the electrical resistance heavily relies on the temperature of a superconducting film. Thus, a large voltage response can be generated by a trifling temperature increase. Therefore, at T_o = 60 K, i.e. closer to the transition temperature, the response more quickly raises from the beginning of the low flux until the flux reaches 100 Wm^{-2} and the response around 42 mV. Notably, when the incident heat flux diminishes, the difference between the voltage responses for a different T_o reduces in a special incident heat flux until the incident energy disappears, whereas for T_o = 50 and 55 K the response curves approximately merge into a common, decreasing line under 40 Wm^{-2}. The result, the voltage response for lower T_o is smaller than that for higher T_o, is again demonstrated in this figure.

From *Figures 5* and *11*, we can infer that the highest incident heat flux can heavily influence the voltage response. Next, we model the type of incident heat flux under a fixed highest flux, 3.81 × 10^7 Wm^{-2}, with varying t_p, i.e. t_p decreases while decreasing the total incident energy, but persists with the same magnitude of the highest incident heat flux, for the different film thermal conductivities, as shown in *Figure 12*. A striking phenomenon is that although the total incident energy decreases, the voltage response is still promoted persistently to a limiting constant as t_p decreases for all different film thermal conductivities. The limiting constants are 10^{-9}, 2 × 10^{-9}, and 5 × 10^{-12} s, respectively, for $k_f/k_{f,YBCO}$ = 1, 0.1, and 0.05. This finding suggests that decreasing the duration to promote the voltage response below the critical pulse duration is futile. The trend of the curve variation implies that under a fixed highest flux, the excess energy of a long pulse duration cannot heighten the performance of a bolometer, but diminish the voltage response. The main reason is a low energy, but that short duration of a pulse induces a more concentrated energy to increase the film temperature, resulting in a prominent response for an operating bolometer. Moreover, when $t_p > 5 \times 10^{-9}$ s, a lower film thermal conductivity causes a larger response, because of poor heat transfer to bring out energy more slowly. In contrast, for a shorter t_p ($< 2 \times 10^{-9}$ s), the fact that there is inadequate time to conduct heat into a substrate before the maximum average temperature has arrived accounts for why a higher film thermal conductivity can more rapidly distribute the energy over the whole film to increase the average film temperature and voltage response. Therefore, a lower film thermal conductivity to reach the limiting voltage response requires a shorter pulse duration for a fixed highest incident heat flux.

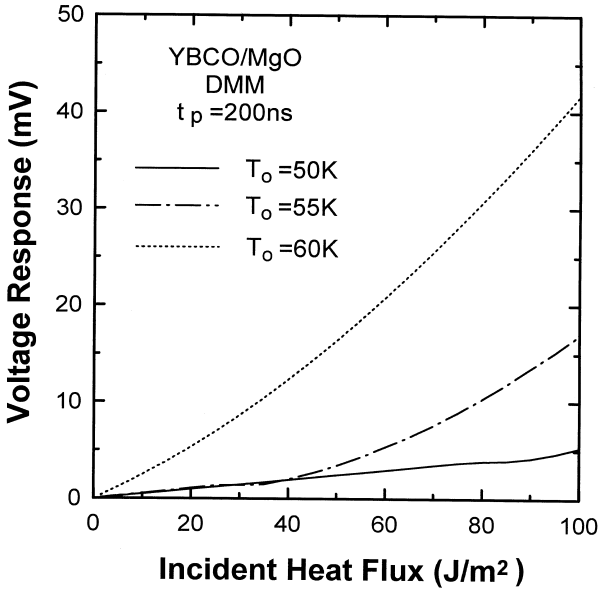

Figure 11 Variation of maximum voltage response with incident heat flux for different initial operating temperatures

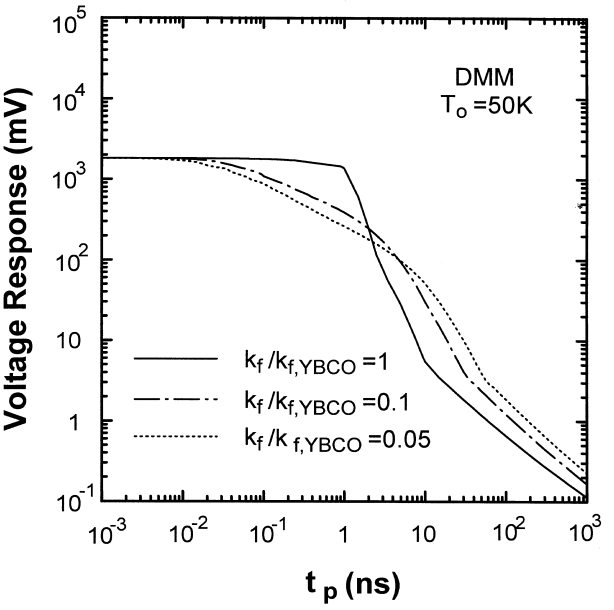

Figure 12 Variation of maximum voltage response with pulse duration under a fixed highest flux for different ratios of thermal conductivity of selected film to YBCO at 50 K

Comparison

Results obtained in this study are compared with the theoretical results of Chen *et al.*[21] and the experimental analysis from Frenkel *et al.*[34], as presented in *Figure 13*. The present result is from the DMM, while the results of Chen *et al.*[21] are from the ILM. A notable phenomenon is that at temperatures near the transition temperature, T_t, both theoretical papers overestimate the experimental value; meanwhile, at temperatures below T_t, both underestimate the value. At temperatures below T_t, the underestimation is reasonable since both thermal models can predict only the bolometric, i.e. the voltage change caused by absorption of radiation. However, there is a non-bolometric effect in the work of Frenkel *et al.* In the non-bolometric mechanism, the voltage response is ascribed to non-linearity in the voltage–current characteristics and is related to the creation of quasiparticle

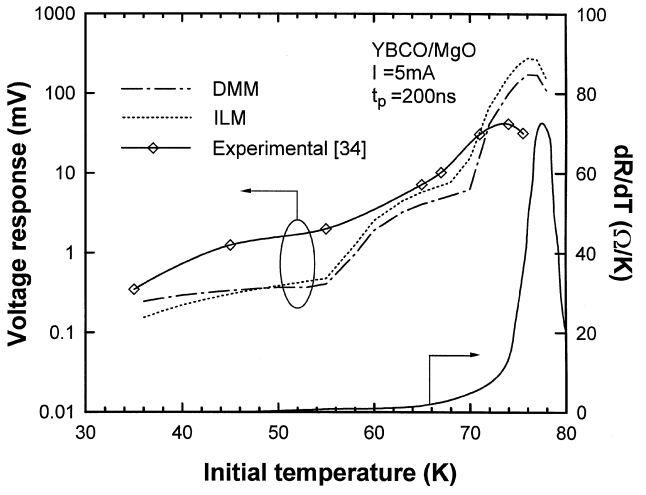

Figure 13 Comparison between the calculated voltage responses for the DMM and the ILM with experimental data[34], and the dependence of dR/dT temperature[34] (right vertical scale) is also shown

pairs induced by incident photons. Only when the non-bolometric part is considered do the theoretical results and experimental results correlate with each other. To our knowledge, this non-bolometric mechanism is still not well understood. Herein, a flux creep model has been employed to study the non-linear characteristics in the low resistivity region; however, the results of this model are questionable. Unlike the underestimation below T_t, the theoretical results overestimate the experimental voltage response at temperatures near T_t. Several possible reasons exist for this overestimation. One is overestimation of the incident heat flux: a higher incident heat flux causes a higher temperature increase and voltage response. Another possible reason is that the energy loss from the front surface is large. The third possible reason is the influence of flux motion. In a high resistivity region, the flux motion changes from flux creep to flux flow. This flux flow mechanism may lead to a lower voltage response than that predicted by the bolometric mechanism. A final possible reason is the hot-electron transport[36]. The initial effect of radiation is to create a number of highly excited electrons and holes at the top of the film. Then the heat rapidly spreads an additional distance of ~ 1 μm via non-equilibrium hot electrons. The hot electrons then thermalize with the lattice, producing an essentially bolometric response.

Two explanations arise as to why the voltage response at temperatures near T_t in this study is lower than that predicted by Chen *et al*.[21]. One explanation is that the thermal boundary resistance from the ILM surpasses that from the DMM, as mentioned in *Figure 4*. At temperatures below ~ 40 K, however, the voltage response found in this study is higher than that reported in Chen *et al*.[21]. This discrepancy is attributed to the fact that the thermal boundary resistance predicted from the DMM exceeds ILM below T ~ 40 K. Notably, all the calculated responses in this work are based on experimentally obtained resistance–temperature curves and "estimated" incident heat fluxes reported in previous experimental investigations. As generally assumed, these curves and incident heat flux values are exact. However, some error due to the uncertainty of measurements can probably not be averted. Thus, a possible reason for the discrepancy between experimental results and theoretical values at temperatures near the transition temperature is the uncertainty of experiments. Further investigations should remedy the discrepancy between theoretical and experimental results.

Conclusions

A thermal analysis of high-T_c superconducting bolometers has been carried out. One-dimensional, variable properties, conjugate film/substrate heat conduction equations with complicated Joule heating have been solved. Three models, the AMM, the DMM, and the ILM, were used to examine the thermal boundary resistance. The thermal boundary resistance is very important for predicting the temperature increase of the bolometer. In general, the voltage response increases with an increase in the thermal boundary resistance or the incident heat flux, whereas the excess energy of a long pulse duration under a fixed highest flux cannot promote the performance of a bolometer. Besides, a shorter or more concentrated energy pulse is favorable for a higher voltage response. The effects of penetration depth are insignificant and only induce a diminutive decrease on voltage response for small penetration depth. In addition, for designing a prominent bolometer, the bolometer formations, the film and the substrate must be selected to be not only both the poor thermal conductivities but also the great specific heat and the thick thickness of the substrate. On the other hand, for short pulse duration a high film thermal conductivity can more rapidly distribute the energy over the whole film to increase the response before the heat conducted into the substrate. From the viewpoint of heat transfer, $SrTiO_3$ (100) or $LaAlO_3$ (100) is a better substrate for fabricating high-T_c superconducting bolometers.

Acknowledgements

The authors wish to express their sincere appreciation to Dr R.C. Chen for his invaluable advice and suggestions during the course of this paper. This research was supported by the National Science Council of the R.O.C. through grant NSC 84-0401-E009-005. The computations were performed on the IBM SP2 at the National Center for High-Performance Computing (NCHC). We are also grateful to the NCHC, because they provide the convenience in numerical calculation.

References

1. Biter, W., Rothwarf, A. and Scoles, K., High-T_c superconductor infrared detectors. *Proceedings of SPIE Conference*, 1989, 1106.
2. Brocklesby, W.S., Monroe, D., Levi, A.F.J., Hong, M., Liou, S.H., Kwo, J., Rice, C.E., Mankiewich, P.M. and Howard, R.E., Electrical response of superconducting $YBa_2Cu_3O_{7-\delta}$ to light. *Appl. Phys. Lett.*, 1989, **54**(12), 1175.
3. Carr, G.L., Quijada, M., Tanner, D.B., Hirschmugl, C.J., Williams, G.P., Etemad, S., Dutta, B., DeRosa, F., Inam, A., Venkatesan, T. and Xi, X., Fast bolometric response by high-T_c detectors measured with subnanosecond synchrotron radiation. *Appl. Phys. Lett.*, 1990, **57**(25), 2725.
4. Forrester, M.G., Gottlieb, M., Gavaler, J.R. and Braginski, A.I., Optical response of epitaxial films of $YBa_2Cu_3O_{7-\delta}$. *Appl. Phys. Lett.*, 1988, **53**(14), 1332.
5. Frenkel, A., Saifi, M.A., Venkatesan, T., England, P., Wu, X.D. and Inam, A., Optical response of non-granular high-T_c $YBa_2Cu_3O_{7-x}$ superconducting thin films. *J. Appl. Phys.*, 1990, **67**, 3054.
6. Kwok, H.S., Zheng, J.P., Ying, Q.Y. and Rao, R., Non-thermal optical response of Y-Ba-Cu-O thin films. *Appl. Phys. Lett.*, 1989, **54**(24), 2473.

7. Oppenheim, U.P., Katz, M., Koren, G., Polturak, E. and Fishman, M.R., High temperature superconducting bolometer. *Physica C*, 1991, **178**, 26.
8. Talvacchio, J., Forrester, M.G. and Braginski, A.I., Photodetection with high-T_c superconducting films of $YBa_2Cu_3O_{7-\delta}$. In *Science and Technology of Thin-Film Superconductors*. Plenum, New York, USA, 1989.
9. Tanabe, K., Kubo, S., Enomoto, Y., Asano, H. and Yamaji, A., Coexistence of bolometric and non-bolometric optical responses in high-T_c $LnBa_2Cu_3O_y$ (Ln = Y,Eu) thin films. *Jap. J. Appl. Phys.*, 1991, **30**(1B), L110.
10. Zeldov, E., Amer, N.M., Koren, G. and Gupta, A., Non-bolometric optical response of $YBa_2Cu_3O_{7-\delta}$ epitaxial films. *Phys. Rev. B*, 1989, **39**(13), 9712.
11. Zheng, J.P., Ying, Q.Y. and Kwok, H.S., Y-Ba-Cu-O thin film infrared detectors. *Physica C*, 1990, **168**, 322.
12. Brasunas, J.C., Moseley, S.H., Lakew, B., Ono, R.H., Mcdonald, D.G., Beall, J.A. and Sauvageau, J.E., Construction and performance of a high-temperature-superconductor composite bolometer. *J. Appl. Phys.*, 1989, **66**(9), 4551.
13. Hu, Q. and Richards, P.L., Design analysis of a high-T_c superconducting microbolometer. *Appl. Phys. Lett.*, 1989, **55**(23), 2444.
14. Richards, P.L., Verghese, S., Geballe, T.H. and Spielman, S.R., The high-T_c superconducting bolometer. *IEEE Trans. Magn.*, 1989, **25**(2), 1335.
15. Verghese, S., Richards, P.L., Char, K. and Sachtjen, S.A., Fabrication of an infrared bolometer with a high-T_c superconducting thermometer. *IEEE Trans. Magn.*, 1991, **27**(2), 3077.
16. Doss, J.D., *Engineering Guide to High-Temperature Superconductivity*, Chapter 4. Wiley, New York, 1989.
17. Chang, K., Yong, G., Wenger, L.E. and Chen, J.T., Observation of non-bolometric response to microwave irradiation on YBaCuO films. *J. Appl. Phys.*, 1991, **69**(10), 7316.
18. Johnson, M., Non-bolometric photoresponse of $YBa_2Cu_3O_{7-\delta}$ films. *Appl. Phys. Lett.*, 1991, **59**(11), 1371.
19. Rose, K., Berlin, C.L. and Katz, R.M., Radiation detectors. *Appl. Supercon.*, 1975, **1**, 267.
20. Uher, C., Thermal conductivity of high-T_c superconductors. *J. Superconductivity*, 1990, **3**(4), 337.
21. Chen, R.C., Wu, J.P. and Chu, H.S., Bolometric response of high-T_c superconducting detectors to optical pulses and continuous waves. *ASME J. Heat Transfer*, 1995, **117**, 336.
22. Streiffer, S.K., Lairson, B.M., Eom, C.B., Clemens, B.M., Bravman, J.C. and Geballe, T.H., Microstructure of ultrathin films of $YBa_2Cu_3O_{7-\delta}$ on MgO. *Phys. Rev. B*, 1991, **43**(16), 13007.
23. Marshall, C.D., Fishman, I.M., Dorfman, R.C., Eom, C.B. and Fayer, M.D., Thermal diffusion, interfacial thermal barrier, and ultrasonic propagation in $YBa_2Cu_3O_7$ thin films: surface-selective transient-grating experiments. *Phys. Rev. B*, 1992, **45**(17), 10009.
24. Little, W.A., The transport of heat between dissimilar solids at low temperatures. *Can. J. Phys.*, 1959, **37**, 334.
25. Swartz, E.T. and Pohl, R.O., Thermal boundary resistance. *Rev. Mod. Phys.*, 1989, **61**, 605.
26. Nahum, M., Verghese, S. and Richards, P.L., Thermal boundary resistance for $YBa_2Cu_3O_{7-\delta}$ films. *Appl. Phys. Lett.*, 1991, **59**(16), 2034.
27. Kumar, S. and Joshi, A., Thermal assessment of a transition-edge high-T_c superconductor infrared detector. *Proceedings of AIAA/ASME Thermophysics and Heat Transfer Conference*. Seattle, Washington, USA, 1990.
28. Flik, M.I., Phelan, P.E. and Tien, C.L., Thermal model for the bolometric response of high-T_c superconducting films to optical pulses. *Cryogenics*, 1990, **30**, 1118.
29. Van Duzer, T. and Turner, C.W., *Principles of Superconductive Devices and Circuits*. Elsevier Press, New York, 1981.
30. Blakemore, J.S., *Solid State Physics*. Cambridge University Press, UK, 1985.
31. Kittel, C., *Introduction to Solid State Physics*. Wiley, New York, USA, 1991.
32. AIP., *American Institute of Physics Handbook*. McGraw–Hill Book Company, New York, 1972.
33. Slack, G.L., Thermal conductivity of MgO, Al_2O_3, $MgAl_2O_4$, and Fe_3O_4 crystals from 3 to 300 K. *Phys. Rev.*, 1962, **126**(2), 427.
34. Frenkel, A., Saifi, M.A., Venkatesan, T., Lin, C., Wu, X.D. and Inam, A., Observation of fast non-bolometric optical response of non-granular high-T_c $YBa_2Cu_3O_{7-x}$ superconducting thin films. *Appl. Phys. Lett.*, 1989, **54**(16), 1594.
35. Hagen, S.J., Wang, Z.Z. and Ong, N.P., Anisotropy of the thermal conductivity of $YBa_2Cu_3O_{7-y}$. *Phys. Rev. B*, 1989, **40**, 9389.
36. Donaldson, W.R., Kadin, A.M., Ballentine, P.H. and Sobolewski, R., Interaction of picosecond optical pulses with high-T_c superconducting films. *Appl. Phys. Lett.*, 1989, **54**(24), 2470.
37. Michael, P.C., Trefny, J.U. and Yarar, B., Thermal transport properties of single crystal lanthanum aluminate. *J. Appl. Phys.*, 1992, **72**(1), 107.
38. Touloukian, Y.S. and Dewitt, D.P., *Thermophysical Properties of Matter*. IFI/Plenum, New York, USA, 1981.
39. Nassau, K. and Miller, A.E., Strontium titanate: an index to the literature on properties and the growth of single crystal. *J. Crystal Growth*, 1988, **91**, 373.